Environmental Science and Pollution Research (2019) 26:28481–28489
https://doi.org/10.1007/s11356-018-3208-3

ALTERNATIVE ADSORBENT MATERIALS FOR APPLICATION IN INDUSTRIAL PROCESSES

Adsorption and removal of chromium (VI) contained in aqueous solutions using a chitosan-based hydrogel

Pâmela Becalli Vilela[1] · Amanda Dalalibera[2] · Eduardo Costa Duminelli[2] · Valter Antonio Becegato[1,2] · Alexandre Tadeu Paulino[1,3]

Received: 20 July 2018 / Accepted: 11 September 2018 / Published online: 18 September 2018

Abstract

The aim of this work was to study the adsorption and removal of chromium (VI) ions contained in aqueous solutions using a chitosan-based hydrogel synthesized via chemical crosslinking of radical chitosan, polyacrylic acid, and *N*,*N*′-methylenebisacrylamide. Fourier-transform infrared spectroscopy confirmed the hydrogel synthesis and presence of reactive functional groups for the adsorption of chromium (VI) ions. The chromium (VI) adsorption mechanism was evaluated using non-linear Langmuir, Freundlich, Redlich-Peterson, and Sips isotherms, with the best fit found by the non-linear Redlich-Peterson isotherm. The maximum chromium (VI) adsorption capacities of the chitosan-based hydrogel were 73.14 and 93.03 mg metal per g dried hydrogel, according to the non-linear Langmuir and Sips isotherm models, respectively. The best kinetic fit was found with the pseudo-nth order kinetic model. The chromium (VI) removal percentage at pH 4.5 and 100 mg L^{-1} initial metal concentration was 94.72%. The results obtained in this contribution can be useful for future works involving scale-up of a water and wastewater treatment method from a pilot plant to full-scale plant.

Keywords Chromium (VI) · Removal · Hydrogel · Chitosan · Adsorption isotherms · Kinetic models

Introduction

Chromium is a chemical species rarely found in natural water, and its presence can be an indicative of environmental pollution caused by electroplating, pigment production, metal plating, dyeing, wood-preserving industries, and so forth (Ravikumar et al. 2015; Deng et al. 2018). Although chromium exists in several oxidation states, the most common species are the chromium (VI) [Cr (VI)] and chromium (III) [Cr (III)] (Wan et al. 2018). Cr (VI) is mutagenic and carcinogenic to humans and highly toxic to animals and plants (Chen et al. 2018; Choudhary and Paul 2018; Pang et al. 2018). The Cr (VI) concentration in drinking water used for human consumption may not be higher than 0.050 mg L^{-1}, and the maximum permitted concentration in water and wastewater for the final disposal in the environment is 0.10 mg L^{-1} (USEPA 2012).

Several methods have been developed and applied for the removal of heavy metals contained in aqueous solutions, including chemical precipitation, ionic exchange, filtration membrane, oxidation-reduction process, dialysis, electrodialysis, and electrolytic extraction (Aslani et al. 2018; Li et al. 2018). However, some of these methods are infeasible for the removal of certain chromium species due to their recalcitrant properties. Moreover, most of the developed methods have high cost, formation of secondary pollutants, high energy consumption, long processing times, poor adsorbent regeneration, and low chromium removal percentage (Li et al. 2018; Wan et al. 2018). Therefore, it is necessary to develop alternative methods for the removal of Cr (VI) ions contained in water and industrial wastewater.

The methods for the removal of heavy metals contained in aqueous solutions based on adsorption are simple, inexpensive,

The original version of this article was revised: The original publication of this paper contains an error. The correct 4th heading in Table 1 should be "Non-linear sips isotherm".

Responsible editor: Tito Roberto Cadaval Jr

✉ Alexandre Tadeu Paulino
alexandre.paulino@udesc.br

[1] Postgraduate Program in Environmental Science, Santa Catarina State University, Av. Luiz de Camões, 2090, Conta Dinheiro,, Lages, SC CEP: 88520-000, Brazil

[2] Department of Environmental and Sanitary Engineering, Santa Catarina State University, Av. Luiz de Camões, 2090, Conta Dinheiro,, Lages, SC CEP: 88520-000, Brazil

[3] Department of Food and Chemical Engineering, Santa Catarina State University, BR 282, km 574,, Pinhalzinho, SC CEP 89870-000, Brazil

effective, and easy to operate and access (Vieira et al. 2018). In general, the adsorbents used for the adsorption and removal of heavy metals contained in water and wastewater need to be inexpensive, biodegradable, and non-toxic (Zhu et al. 2017). In this case, the most common adsorbents include zeolites, clays, silicates, biomass, polymers, hydrogels, composites, and so forth (Pereira et al. 2017; Vieira et al. 2018). Natural polysaccharide-based hydrogels are adsorbents formed by hydrophobic/hydrophilic three-dimensional polymer networks capable of absorbing large amounts of water. Hence, these adsorbents can be efficiently employed for the adsorption of dyes, proteins, agricultural nutrients, and heavy metals (Vieira et al. 2018).

The aim of this work was to study the adsorption and removal of Cr (VI) ions contained in aqueous solutions using a chitosan-based hydrogel as alternative adsorbent. These studies were performed at different contact times, pH, and initial metal concentrations. The Cr (VI) adsorption mechanism in the hydrogel was evaluated using non-linear Langmuir, Freundlich, Redlich-Peterson, and Sips isotherms, whereas the Cr (VI) adsorption kinetic was evaluated using non-linear pseudo-first, pseudo-second, and pseudo-*n*th order kinetic models.

Materials and methods

Reagents

Chitosan from shrimp (CS—deacetylation degree: 92.0 wt-%; 1.0×10^6 Da molar mass and 425 μm particle size), ammonium persulfate (APS), *N*,*N*′-methylenebisacrylamide (MBA), and acrylic acid (AA) were purchased from Aldrich®. Hydrochloridric acid and acetic acid (AAc) were purchased from Merck®. Sodium hydroxide (NaOH) and potassium dichromate ($Cr_2K_2O_7$) were purchased from Dinamica®. All reagents were used as acquired and aqueous solutions were prepared in ultrapure water (Megapurity MEGA-UP).

Hydrogel synthesis

The chitosan-based hydrogel was synthesized by placing 30.0 mL of 1.0 wt-% CS solution, 3.40 mL of AA, 0.150 g of MBA, and 0.5215 mmol of APS (initiator) in a three-neck glass flask equipped with a mechanical stirrer, reflux condenser, and nitrogen line. The hydrogel synthesis was performed at 343.15 K for 3 h under inert atmosphere for complete crosslinking. The formed hydrogel was transferred to a 200.0-mL glass beaker containing 100.0 mL of 2.0 mol L^{-1} sodium hydroxide solution and left for 15 min to neutralize. Finally, the hydrogel was washed with ultrapure water and dried in an air circulation oven (Ethiktechnology 400/5TS) at 333.15 K for 72 h prior to characterization and application for the adsorption and removal of Cr (VI) ions contained in aqueous solutions.

Fourier-transform infrared spectroscopy

Fourier-transform infrared spectroscopy (FT-IR) was conducted with the Bomem Easy MB-100 Nichelson spectrometer. The hydrogel sample was prepared using 1.0 wt-% KBr pellets and FTIR spectra obtained with 20 runs per minute at resolution of 4.0 cm^{-1}.

Adsorption experiments

The Cr (VI) adsorption experiments were performed using 1000 mg L^1 stock metal solutions at pH 4.5, 5.5, and 6.5. Dried hydrogel masses (100.0 mg) were immersed in 120.0-mL glass Erlenmeyer flasks containing 50.0 mL of Cr (VI) ion aqueous solutions at specific initial concentrations. The Cr (VI) concentrations were determined via flame atomic absorption spectrometry (FAAS—Analytic Jena AG, Jena, Germany, contra 700, air-acetylene flame, wavelength for chromium of 357.8687 nm). The removal percentage (R, %) was calculated using Eq. (1):

$$\mathrm{R},\% = \frac{\mathbf{C_0} - \mathbf{C_e}}{\mathbf{C_0}} 100 \tag{1}$$

in which $\mathbf{C_0}$ and $\mathbf{C_e}$ are the initial and equilibrium concentrations (mg L^{-1}), respectively.

The Cr (VI) adsorption capacities (q_e, mg g^{-1}) of the hydrogel were calculated using Eq. (2):

$$q_e = \frac{C_0 - C_e}{m} V \tag{2}$$

in which m (g) is the dried hydrogel mass and V (mL) is the aqueous solution volume.

Adsorption isotherms

The Langmuir isotherm model is employed to explain the monolayer adsorption mechanism occurring at a defined number of active sites on the hydrogel network (Langmuir 1916). On the contrary, the Freundlich isotherm model is employed to explain the multilayer adsorption mechanism occurring on heterogeneous surfaces, with intermolecular interactions among adsorbed ions on neighbor active sites (Freundlich 1906). The three-parameter Redlich-Peterson and Sips isotherm models are employed to study homogeneous and heterogeneous adsorption systems (Foo and Hameed 2010). The Redlich-Peterson isotherm model describes the adsorption occurring with monolayer formation and multi-site interactions simultaneously (Redlich and Peterson 1959), whereas the Sips isotherm model describes the adsorption occurring only on

heterogeneous systems (Sips 1948). The non-linear Langmuir, Freundlich, Redlich-Peterson, and Sips isotherm models are represented by Eqs. (3), (4), (5), and (6), respectively:

$$q_e = \frac{q_{max} K_L C_e}{1 + K_L C_e} \tag{3}$$

in which q_e (mg g^{-1}) is the adsorption capacity of the hydrogel, q_{max} (mg g^{-1}) is the maximum adsorption capacity, K_L (L mg^{-1}) is the Langmuir adsorption constant, and C_e (mg L^{-1}) is the metal concentration at equilibrium:

$$q_e = K_F C_e^{\frac{1}{n}} \tag{4}$$

in which K_F (mg g^{-1}) is the Freundlich constant related with the adsorption capacity and $1/n$ is the Freundlich constant related with the surface heterogeneity of the specific adsorbate.

$$q_e = \frac{K_R C_e}{1 + a_R C_e^{\beta}} \tag{5}$$

in which a_R (mg^{-1}) and K_R (L g^{-1}) are the Redlich-Peterson constants, and β is an exponent having values between 0 and 1:

$$q_e = \frac{q_{ms} K_s C_e^{\beta_S}}{1 + K_S C_e^{\beta_S}} \tag{6}$$

in which q_{ms} (mg g^{-1}) is the maximum Sips adsorption capacity, K_s (L mg^{-1}) is the Sips constant at equilibrium, and β_S is the Sips exponent describing the homogeneity and heterogeneity of an adsorption mechanism.

Adsorption kinetics

Kinetic studies are employed to evaluate the adsorption dynamic with base on the rate constants (Norouzi et al. 2018). The steps of an adsorption process are governed by (i) transport of solute from the solution bulk to a thin film formed on the adsorbent surface, (ii) transport of solute from this thin film to the adsorbent surface, and (iii) transport of solute from the adsorbent surface to the interior of the porous structure (Sharma and Bhattacharyya 2005). The Cr (VI) adsorption kinetics in the chitosan-based hydrogel were studied using non-linear pseudo-first, pseudo-second, and pseudo-*n*th order kinetic models. The non-linear pseudo-first and pseudo-second order kinetic models are represented by Eqs. (7) and (8), respectively:

$$q_t = q_e\left(1 - e^{-kt}\right) \tag{7}$$

$$q_t = \frac{k q_e^2 t}{1 + k q_e t} \tag{8}$$

The non-linear pseudo-nth order kinetic model is represented by Eq. (9):

$$q_t = q_e - \left[(n-1)kt + q_e^{(1-n)}\right]^{\frac{1}{1-n}} \tag{9}$$

in which k (min^{-1}) is the adsorption rate, t (mim) is the adsorption time, q_t (mg g^{-1}) is the adsorption capacity at adsorption time t, and n is the reaction order with regard to the effective concentration.

Error analysis

The experimental data obtained from the Cr (VI) adsorption isotherms and kinetics in the chitosan-based hydrogel were evaluated using chi-square test statistic (χ^2) (Tang et al. 2018) which is represented by Eq. (10):

$$\chi^2 = \sum \frac{\left(q_{experimental} - q_{e,theoretical}\right)^2}{q_{e,theoretical}} \tag{10}$$

The coefficient of determination (R^2) based on the chi-square test statistic is represented by Eq. (11):

$$R^2 = \frac{\sum\left(q_{e,theoretical} - \overline{q_e}\right)^2}{\sum\left(q_{e,theoretical} - \overline{q_e}\right)^2 + \sum\left(q_{e,theoretical} - q_{experimental}\right)^2} \tag{11}$$

in which $q_{e,theoretical}$ and $q_{experimental}$ are the theoretical adsorption capacities (mg g^{-1}) predicted from each model and experimental adsorption capacities (mg g^{-1}) calculated from the experimental adsorption results, respectively. $\overline{q_e}$ (mg g^{-1}) is the average of $q_{experimental}$.

Results and discussion

Fourier-transform infrared spectroscopy

Figure 1a shows a Fourier-transform infrared spectrum for the chitosan-based hydrogel. The absorption bands at 3400 and 3200 cm^{-1} are attributed to stretching vibrations of O–H and N–H groups, respectively, from CS molecules. The absorption band at 3400 cm^{-1} can also be attributed to stretching vibrations of O–H groups from AA molecules. The absorption band at 2925 cm^{-1} is related to the vibrations of aliphatic compounds containing C–H groups. Carbonyl groups (C=O) are frequently observed at absorption bands from 1820 to 1680 cm^{-1} (He et al. 2015; Falamarzpour et al. 2017). Hence, the absorption band at 1750 cm^{-1} indicates the presence of C=O groups from polyacrylic acid (PAA), MBA, and radical CS. The absorption bands between 1500 and

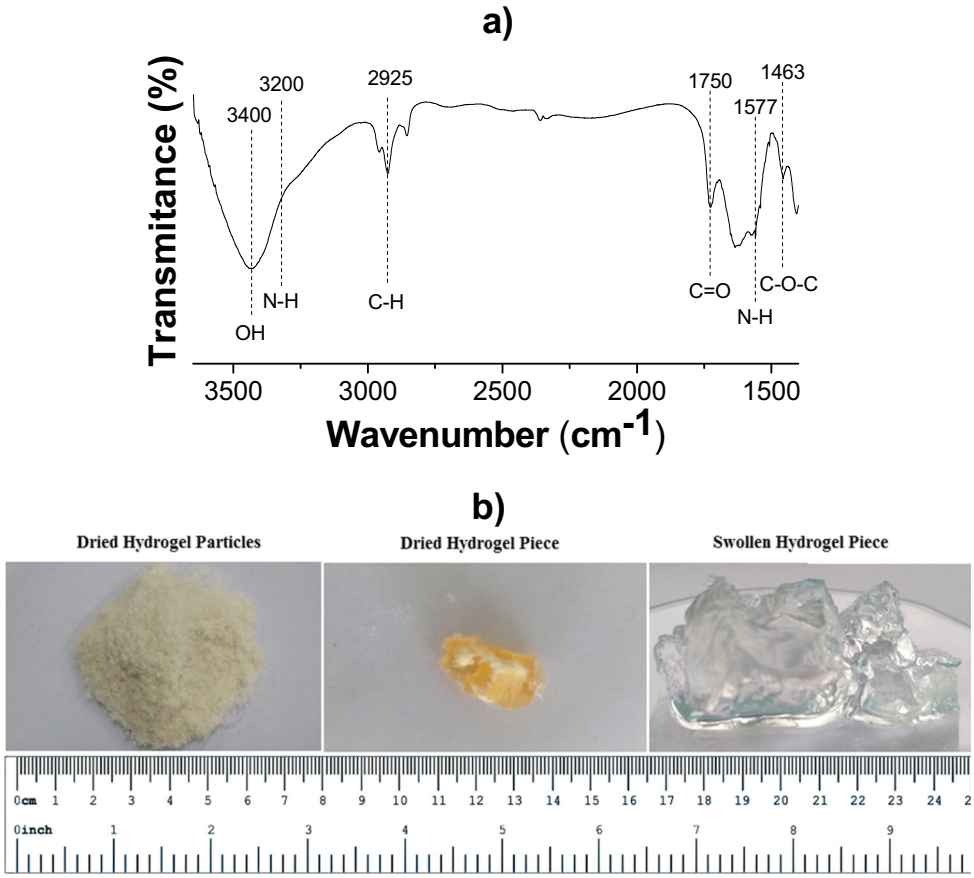

Fig. 1 **a**, **b** Fourier-transform infrared spectrum for the chitosan-based hydrogel (**a**). Photos of the dried hydrogel particles, dried hydrogel piece, and swollen hydrogel piece (**b**)

1600 cm^{-1} are associated with primary and secondary amide groups due to occurrence of crosslinking reactions involving high deacetylation-degree chitosan (Li and Tang 2016; Falamarzpour et al. 2017; Mohamed and El-Ghany 2017). The absorption band at 1577 cm^{-1} is related to the stretching deformation of N–H groups from CS and MBA molecules. Finally, the absorption band at 1463 cm^{-1} is related to the stretching of C–O–C groups.

Other characterizations

Scanning electron microscopy (SEM) images for the chitosan-based hydrogel were recently published by our research group (Varnier et al. 2018). Mechanical properties were confirmed by the values of the modulus of elasticity (0.30 kPa) and applied compression force (0.38 N). Photos of dried hydrogel particles, dried hydrogel piece, and swollen hydrogel piece are shown in Fig. 1b.

Effect of contact time and pH

Figure 2 shows the Cr (VI) adsorption capacities of the chitosan-based hydrogel versus time at pH 4.5, 5.5, and 6.5. The Cr (VI) adsorption capacities were 47.36, 43.90, and 40.79 mg metal per g dried hydrogel at pH 4.5, 5.5, and 6.5, respectively, after 1440 min. The high initial adsorption rates are results of the high amounts of available active sites in the hydrogel. These adsorption rates decreased with the increase of the contact time due to partial saturation of the active sites. It confirms that the adsorption kinetic depends on the adsorbate rate transported from the solution bulk to the adsorbent surface

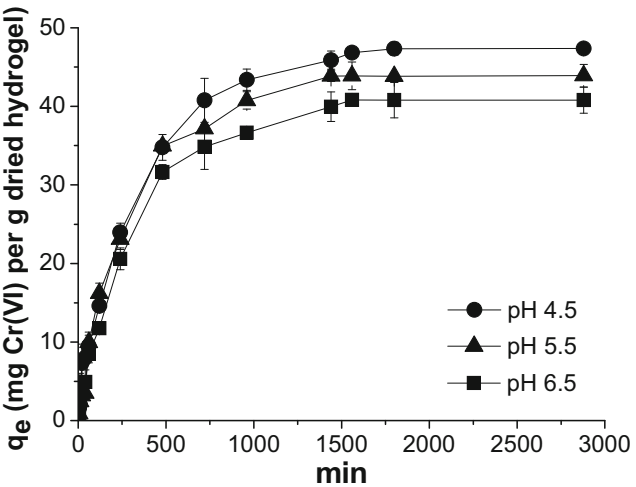

Fig. 2 Cr (VI) adsorption capacities of the chitosan-based hydrogel versus time at pH 4.5, 5.5, and 6.5. Experimental conditions 100.0 mg L^{-1} initial metal concentration, 100.0 mg hydrogel mass and room temperature

(Nascimento et al. 2014). The Cr (VI) adsorption capacity increased with the decrease of pH due to changes in the ionic network of the chitosan-based hydrogel (Paulino et al. 2011a) and formation of specific Cr (VI) species in aqueous solutions at different pH values (Wan et al. 2018). The COO^- and NH_2 groups contained in the hydrophilic three-dimensional network of the chitosan-based hydrogel are protonated at pH values lower than 6.0, forming COOH and NH_3^+. This decreases the intermolecular interaction forces between Cr (VI) ions and active sites. However, the high H^+ ion concentration can be predominant to form significant amounts of either NH_3^+ or NH_4^{2+} and increase the electrostatic attraction forces between NH_3^+ or NH_4^{2+} and chromate (CrO_4^{-2}), dichromate ($Cr_2O_7^{-2}$), hydrogen chromate ($HCrO_4^-$), and hydrogen dichromate ($HCr_2O_7^-$) (Luz and Oliveira 2011; Ba et al. 2018). $HCrO_4^-$ ions are considered the main ionic forms of chromium at pH from 2.0 to 6.4, whereas CrO_4^{-2} ions are considered the main ionic forms of chromium at pH higher than 6.4. Hence, higher $HCrO_4^-$ ion concentrations were adsorbed at lower pH values, increasing the Cr (VI) adsorption capacities of the hydrogel (Chai et al. 2018).

Effect of initial Cr (VI) concentration at different pH values

Figure 3 shows the Cr (VI) adsorption capacities of the chitosan-based hydrogel versus pH at initial metal concentrations from 100.0 to 400.0 mg L^{-1}. The Cr (VI) adsorption capacities ranged from 47.36 to 75.80 mg metal per g dried hydrogel with the increase in the initial metal concentration from 100.0 to 400.0 mg L^{-1}, respectively, at pH 4.5. The Cr (VI) adsorption capacities ranged from 43.90 to 60.85 mg metal per g dried hydrogel, respectively, at pH 5.5 and 40.79 to 23.63 mg metal per g dried hydrogel, respectively, at pH 6.5. The Cr (VI) adsorption capacities decreased with the increase of pH due to the decrease of the $HCrO_4^-$ ion concentrations in aqueous solution and cationic group concentrations in the hydrophilic three-dimensional network of the chitosan-based hydrogel. Moreover, the increase of pH increased the electrostatic repulsion forces among CrO_4^{-2}, $Cr_2O_7^{-2}$, $HCrO_4^-$, and $HCr_2O_7^-$ ions and carboxylate groups (COO^-) in the hydrogel network (Paulino et al. 2011a), decreasing the adsorption capacities. The stronger intermolecular interaction forces that occurred between $HCrO_4^-$ ions and cationic groups, at pH lower than 6.0, overcame the lower degrees of swelling of the chitosan-based hydrogel (Vieira et al. 2018), increasing the Cr (VI) adsorption capacities. The Cr (VI)

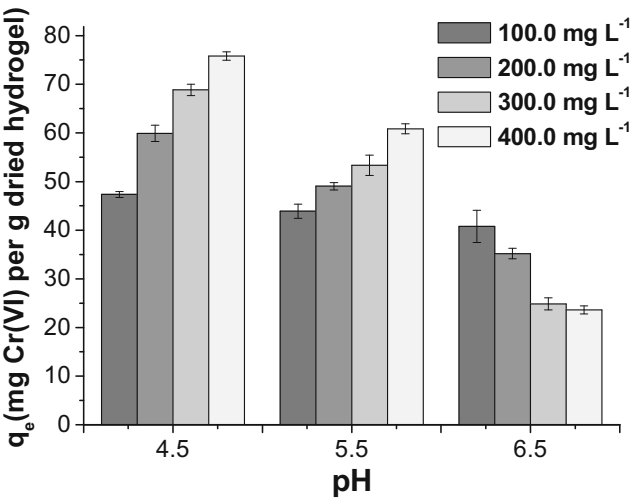

Fig. 3 Cr (VI) adsorption capacities of the chitosan-based hydrogel versus initial metal concentration at pH 4.5, 5.5, and 6.5. Experimental conditions contact time of 2880 min; initial metal concentration from 100.0 to 400.0 mg L^{-1}; 100.0 mg adsorbent mass; 50.0 mL solution volume and room temperature

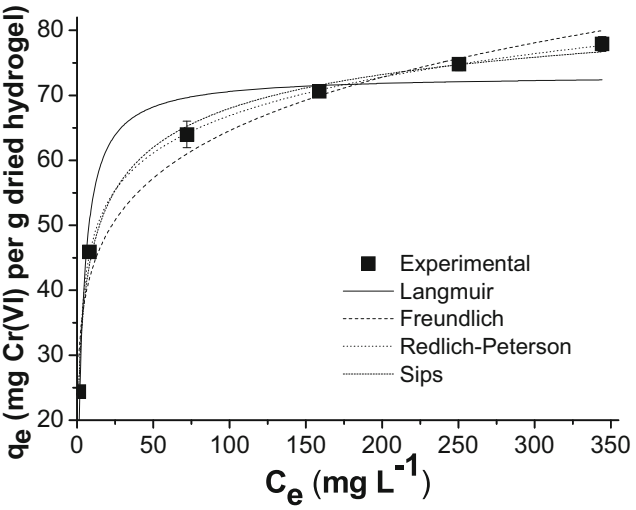

Fig. 4 Non-linear Langmuir, Freundlich, Redlich-Peterson and Sips isotherms for the adsorption of Cr (VI) ions to the chitosan-based hydrogel. Experimental conditions: contact time of 1440 min; initial metal concentration from 50.0 to 500.0 mg L^{-1}; 100.0 mg adsorbent mass; 50.0 mL solution volume; pH 4.5 and room temperature

Table 1 Parameters of the non-linear Langmuir, Freundlich, Redlich-Peterson, and Sips isotherms for the adsorption of Cr(VI) ions to the chitosan-based hydrogel

Non-linear Langmuir isotherm				
R^2	K_L (L mg^{-1})	q_{max} (mg g^{-1})		χ^2
0.9173	0.277	73.14		35.26
Non-linear Freundlich isotherm				
R^2	K_F (mg g^{-1})	n		χ^2
0.9654	29.11	5.780		14.77
Non-linear Redlich-Peterson isotherm				
R^2	a_R (mg^{-1})	K_R (L g^{-1})	β	χ^2
0.9999	1.343	53.73	0.886	0.064
Non-linear sips isotherm				
R^2	β_S	K_S (L mg^{-1})	q_{ms} (mg g^{-1})	χ^2
0.9934	0.443	0.354	93.03	2.814

Table 2 Maximum Cr(VI) adsorption capacities of the chitosan-based hydrogel compared to other adsorbent materials studied at different pH values

Adsorbent	Initial pH	q_{max} (mg g^{-1})	Reference
Clinoptilolite	2.0	10.42	Jorfi et al. (2017)
Anthill-eggshell composite (AEC)	4.5	12.99	Yusuff et al. (2018)
Eucalyptus bark biochar (EBB)	2.0	21.30	Choudhary and Paul (2018)
Polyaniline coated chitin	4.2	24.60	Karthik and Meenakshi (2015)
Pomelo peel activated biochar (PPAB)	2.0	57.64	Wu et al. (2017)
Peanut hull magnetic biochar	5.1	77.54	Han et al. (2016)
Chitosan-based hydrogel	4.5	93.03	This study

removal percentage from an aqueous solution with pH 4.5 and 100.0 mg L^{-1} initial metal concentration was 94.72%. The Cr (VI) removal capacities and percentages increased with the increase of the initial metal concentrations at pH 4.5 and 5.5 up to saturation of the active sites in the hydrogel network. Otherwise, the Cr (VI) removal capacities and percentages decreased with the increase of the initial metal concentration at pH 6.5. This indicates that the CrO_4^{-2} ion affinity by active sites in the chitosan-based hydrogel, at higher pH values, is lower than $HCrO_4^-$ ion affinity, which predominates in more acidic solutions (Wan et al. 2018).

Adsorption isotherms

Figure 4 shows the results of the non-linear Langmuir, Freundlich, Redlich-Peterson, and Sips isotherms for the adsorption of Cr (VI) ions to the chitosan-based hydrogel. Table 1 shows the isotherm parameters. The best fits for the adsorption of Cr (VI) ions were obtained using the non-linear Redlich-Peterson and Sips isotherm models, with higher R^2 value and lower chi-square test statistic (χ^2) for the non-linear Redlich-Peterson isotherm. It indicates that the adsorption of Cr (VI) ions is governed by formation of monolayer and multi-site interactions concomitantly, modifying the hydrogel structure (Vieira et al. 2018; Paulino et al. 2011b). As the exponent β of the non-linear Redlich-Peterson isotherm model was not equal to 1, the adsorption process is not exclusively governed by the Langmuir isotherm (Redlich and Peterson 1959). Hence, the maximum Cr (VI) adsorption capacity should be better represented by the non-linear Sips isotherm model. The maximum Cr (VI) adsorption capacities of the chitosan-based hydrogel were 73.14 and 93.03 mg metal per g dried hydrogel, according to the non-linear Langmuir and Sips isotherm models, respectively. The maximum Cr (VI)

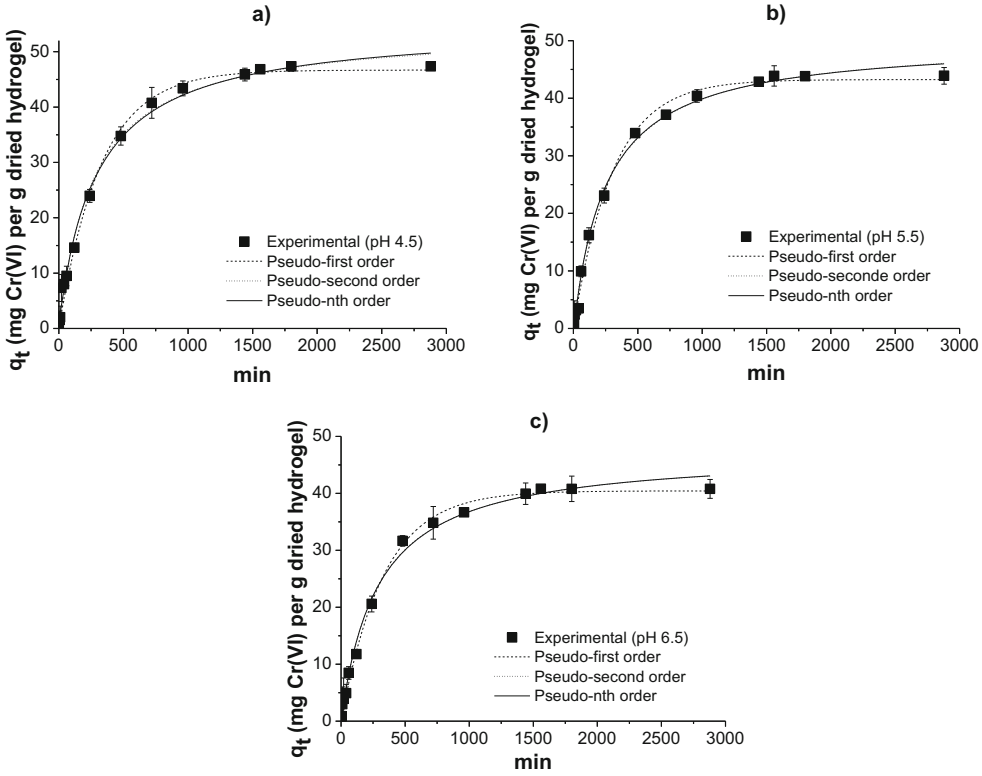

Fig. 5 Non-linear pseudo-first, pseudo-second, and pseudo-*n*th-order kinetic models for the adsorption of Cr (VI) ions to the chitosan-based hydrogel at pH 4.5 (**a**), 5.5 (**b**), and 6.5 (**c**). Experimental conditions: 100.0 mg L^{-1} initial metal concentration; 100.0 mg adsorbent mass; 50.0 mL solution volume and room temperature

Table 3 Parameters of the non-linear pseudo-first, pseudo-second and pseudo-*n*th order kinetic models for the adsorption of Cr(VI) ions to the chitosan-based hydrogel at different pH values

Pseudo-first order				
pH	R^2	K_1 (min^{-1})	q_e (mg g^{-1})	χ^2
4.5	0.9930	3.080×10^{-3}	46.68	2.663
5.5	0.9957	3.270×10^{-3}	43.24	1.514
6.5	0.9967	3.020×10^{-3}	40.44	1.007
Pseudo-second order				
pH	R^2	K_2 (min^{-1})	q_e (mg g^{-1})	χ^2
4.5	0.9942	6.788×10^{-5}	54.22	2.193
5.5	0.9958	7.656×10^{-5}	50.21	1.460
6.5	0.9951	7.391×10^{-5}	47.32	1.454
Pseudo-*n*th order				
pH	R^2	K_n (min^{-1}) (mg g^{-1})	*n*	q_e (mg g^{-1})	χ^2
4.5	0.9947	6.324×10^{-5}	1.998	54.74	2.051
5.5	0.9956	7.873×10^{-5}	2.000	50.03	1.526
6.5	0.9948	7.309×10^{-5}	1.999	47.39	1.560

adsorption capacities of the chitosan-based hydrogel were compared to the adsorption capacities of other adsorbent materials studied at different pH values as shown in Table 2. As it can be seen, the chitosan-based hydrogel could be efficiently applied for the removal of Cr (VI) ions contained in aqueous solutions compared to some adsorbent materials.

Adsorption kinetics

Figure 5 shows the experimental and predicted results of the non-linear pseudo-first, pseudo-second, and pseudo-*n*th order kinetic models for the adsorption of Cr (VI) ions to the chitosan-based hydrogel at pH 4.5 (a), 5.5 (b), and 6.5 (c). Table 3 shows the parameters of the non-linear pseudo-first, pseudo-second, and pseudo-*n*th order kinetic models. The best kinetic fit for the adsorption of Cr (VI) ions to the chitosan-based hydrogel at pH 4.5 was obtained using the non-linear pseudo-*n*th order kinetic model, with higher R^2 value and lower chi-square test statistic (χ^2). However, the adsorption kinetics changed with the increase of pH since the best kinetic

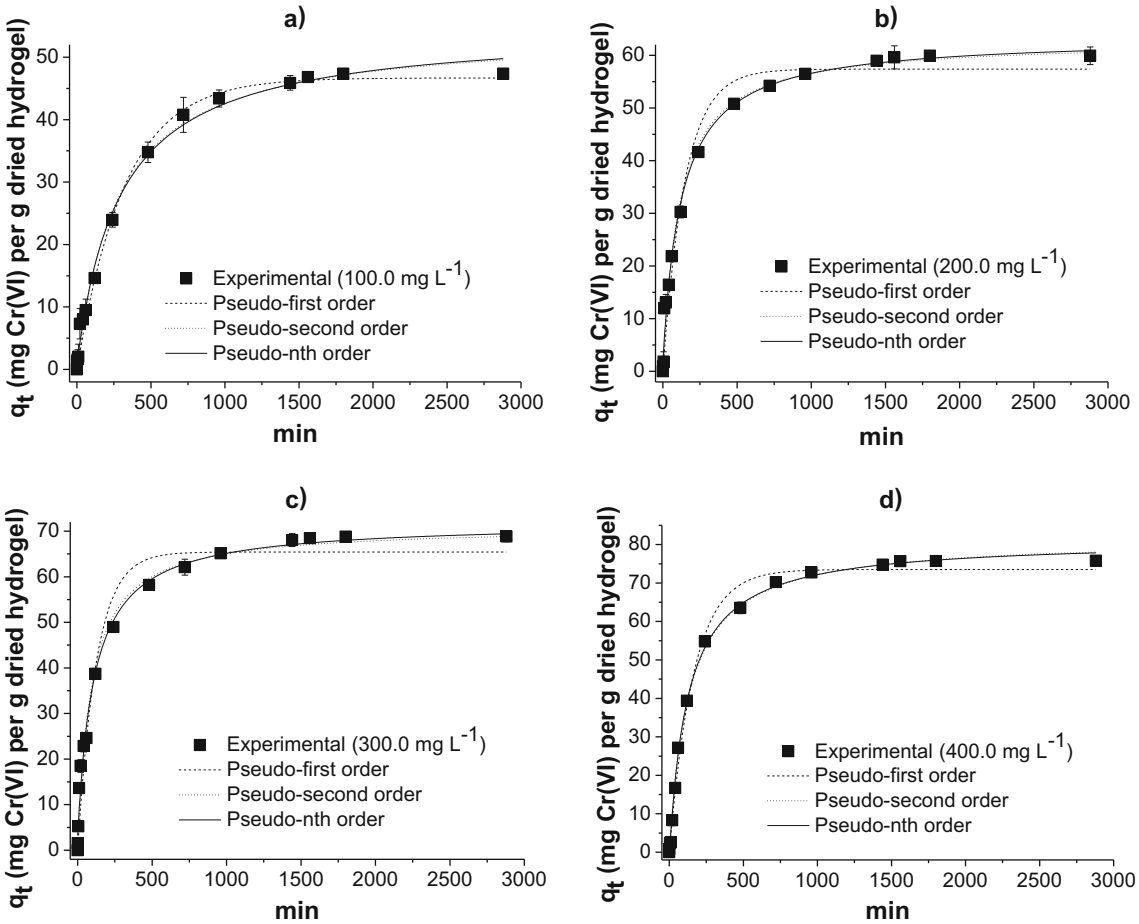

Fig. 6 Non-linear pseudo-first, pseudo-second, and pseudo-*n*th-order kinetic models for the adsorption of Cr (VI) ions to the chitosan-based hydrogel at initial metal concentrations of 100.0 (**a**), 200.0 (**b**), 300.0 (**c**), and 400.0 mg L^{-1} (**d**). Experimental conditions: 100.0 mg adsorbent mass; 50.0 mL solution volume; pH 4.5 and room temperature

Table 4 Parameters of the non-linear pseudo-first, pseudo-second, and pseudo-*n*th-order kinetic models for the adsorption of Cr(VI) ions to the chitosan-based hydrogel at different initial metal concentrations (C_0)

Pseudo-first order				
C_0 (mg L^{-1})	R^2	K_1 (min^{-1})	q_e (mg g^{-1})	χ^2
100.0	0.9931	3.080×10^{-3}	46.68	2.663
200.0	0.9767	6.710×10^{-3}	57.36	13.31
300.0	0.9705	7.970×10^{-3}	65.43	21.16
400.0	0.9938	6.100×10^{-3}	73.54	6.343
Pseudo-second order				
C_0 (mg L^{-1})	R^2	K_2 (min^{-1})	q_e (mg g^{-1})	χ^2
100.0	0.9943	6.788×10^{-5}	54.22	2.193
200.0	0.9914	1.437×10^{-4}	62.82	4.897
300.0	0.9890	1.539×10^{-4}	71.01	7.918
400.0	0.9974	9.352×10^{-5}	81.62	2.686
Pseudo-*n*th order				
C_0 (mg L^{-1})	R^2	K_n (min^{-1}) (mg g^{-1})	n	q_e (mg g^{-1})	χ^2
100.0	0.9947	6.324×10^{-5}	1.998	54.74	2.051
200.0	0.9926	1.285×10^{-4}	1.996	63.46	4.202
300.0	0.9918	1.311×10^{-4}	1.995	71.98	5.916
400.0	0.9978	9.873×10^{-5}	2.002	81.22	2.293

fit at pH 6.5 was found with the non-linear pseudo-first order kinetic model when comparing R^2 and χ^2. This confirms that CrO_4^{-2} ions predominate at less acidic solutions. As the reaction order (n) was approximately 2 at pH 4.5, both non-linear pseudo-*n*th and pseudo-second-order kinetic models can be used to fit the experimental adsorption data (Guechi and Hamdaoui 2013). The best kinetic fit for the adsorption of Cr (VI) ions to the chitosan-based hydrogel at pH 5.5 was found with the pseudo-second-order kinetic model, confirming the reaction order ($n = 2.000$). This suggests that the adsorptions of different chromium species to the chitosan-based hydrogel are governed by the active-binding site number (Norouzi et al. 2018). Overall, the adsorption of Cr (VI) ions to the chitosan-based hydrogel is more favorable at lower pH values.

Figure 6 shows the experimental and predicted results of the non-linear pseudo-first, pseudo-second, and pseudo-*n*th-order kinetic models for the adsorption Cr (VI) ions to the chitosan-based hydrogel at initial metal concentrations of 100.0 (a), 200.0 (b), 300.0 (c), and 400.0 mg L^{-1} (d). Table 4 shows the parameters of the non-linear pseudo-first, pseudo-second, and pseudo-*n*th-order kinetic models. All coefficients of determination (R^2) were higher, and chi-square test statistics (χ^2) were lower when using the non-linear pseudo-*n*th-order kinetic model, independently of the initial Cr (VI) concentration. Hence, the best kinetic fits for the adsorption of Cr (VI) ions to the chitosan-based hydrogel at all initial concentrations were found with the non-linear pseudo-*n*th-order kinetic model. Moreover, the calculated and predicted q_e values were similar to the q_e values determined experimentally during the adsorption of Cr (VI) ions, confirming that the best fit was found with the non-linear pseudo-*n*th-order kinetic model. These results can be employed for confirming a favorable Cr (VI) adsorption process in hydrogels.

Conclusion

- A chitosan-based hydrogel could be efficiently employed as alternative adsorbent for the adsorption and removal of Cr (VI) ions contained in aqueous solutions.
- The best fit for the adsorption of Cr (VI) ions to the chitosan-based hydrogel was found with the non-linear Redlich–Peterson isotherm model.
- The Cr (VI) adsorption mechanism was governed by formation of monolayer and multi-site interactions concomitantly.
- The best kinetic fit for the adsorption of Cr (VI) ions to the chitosan-based hydrogel was found with the non-linear pseudo-*n*th-order kinetic model.
- A chitosan-based hydrogel could be efficiently applied as cost-effective and eco-friendly alternative adsorbent for the water and wastewater treatment containing heavy metals.

Acknowledgements ATP and PBV thank the Brazilian fostering agency CAPES for the master scholarship.

Funding information

Brazilian fostering agency CNPq (Grant N° 312356/2015-3) for provided financial support.

References

Aslani H, Kosari TE, Naseri S, Nabizadeh R, Khazaei M (2018) Hexavalent chromium removal from aqueous solution using functionalized chitosan as a novel nano-adsorbent: modeling and optimization, kinetic, isotherm, and thermodynamic studies, and toxicity testing. Environ Sci Pollut Res 25:20154–20168. https://doi.org/10.1007/s11356-018-2023-1

Ba S, Alagui A, Hajjaji M (2018) Retention and release of hexavalent and trivalent chromium by chitosan, olive stone activated carbon, and their blend. Environ Sci Pollut Res 25:19585–19604. https://doi.org/10.1007/s11356-018-2196-7

Chai Q, Lu L, Lin Y, Ji X, Yang C, He S, Zhang D (2018) Effects and mechanisms of anionic and nonionic surfactants on biochar removal of chromium. Environ Sci Pollut Res 25:18443–18450. https://doi.org/10.1007/s11356-018-1933-2

Chen H, Guo Z, Zhou Y, Li D, Mu L, Klerks PL, Luo Y, Xie L (2018) Accumulation, depuration dynamics and effects of dissolved hexavalent chromium in juvenile Japanese medaka. Ecotox Environ Safe 148:254–260. https://doi.org/10.1016/j.ecoenv.2017.10.037

Choudhary B, Paul D (2018) Isotherms, kinetics and thermodynamics of hexavalent chromium removal using biochar. J Environ Chem Eng 6:2335–2343. https://doi.org/10.1016/j.jece.2018.03.028

Deng X, Qi L, Zhang Y (2018) Experimental study on adsorption of hexavalent chromium with microwave-assisted alkali modified fly ash. Water Air Soil Pollut 229:18. https://doi.org/10.1007/s11270-017-3679-8

Falamarzpour P, Behzad T, Zamani A (2017) Preparation of nanocellulose reinforced chitosan films, cross-linked by adipic acid. Int J Mol Sci 18:396. https://doi.org/10.3390/ijms18020396

Foo KY, Hameed BH (2010) Insights into the modeling of adsorption isotherm systems. Chem Eng J 156:2–10. https://doi.org/10.1016/j.cej.2009.09.013

Freundlich HMF (1906) Over the adsorption in solution. J Phys Chem 57: 385–471

Guechi EK, Hamdaoui O (2013) Cattail leaves as a novel biosorbent for the removal of malachite green from liquid phase: data analysis by non-linear technique. Desalin Water Treat 51(16–18):3371–3380. https://doi.org/10.1080/19443994.2012.749191

Han Y, Cao X, Ouyang X, Sohi SP, Chen J (2016) Adsorption kinetics of magnetic biochar derived from peanut hull on removal of Cr(VI) from aqueous solution: effects of production conditions and particle size. Chemosphere 145:336–341. https://doi.org/10.1016/j.chemosphere.2015.11.050

He G, Xiang C, Yin Y, Cai W, Ke W, Kong Y, Zheng H (2015) Preparation and antibacterial properties of O-carboxymethyl chitosan/lincomycin hydrogels. J Biomater Sci Polym Ed 27:370–384. https://doi.org/10.1080/09205063.2015.1132616

Jorfi S, Ahmadi MJ, Pourfadakari S, Jaafarzadeh N, Soltani RDC, Akbari H (2017) Adsorption of Cr(VI) by natural clinoptilolite zeolite from aqueous solutions: isotherms and kinetics. Pol J chem Tech 19:106–114. https://doi.org/10.1515/pjct-2017-0056

Langmuir I (1916) The constitution and fundamental properties of solids and liquids. Part I. solids. J Am Chem Soc 38:2221–2295. https://doi.org/10.1021/ja02268a002

Karthik R, Meenakshi S (2015) Synthesis, characterization and Cr(VI) uptake study of polyaniline coated chitin. Int J Biol Macromol 72: 235–242. https://doi.org/10.1016/j.ijbiomac.2014.08.022

Li H, Gao P, Cui J, Zhang F, Wang F, Cheng J (2018) Preparation and Cr(VI) removal performance of corncob activated carbon. Environ Sci Pollut Res 25:20743–20755. https://doi.org/10.1007/s11356-018-2026-y

Li XQ, Tang RC (2016) Crosslinking of chitosan fiber by a water-soluble diepoxy crosslinker for enhanced acid resistance and its impact on fiber structures and properties. React Funct Polym 100:116–122. https://doi.org/10.1016/j.reactfunctpolym.2016.01.015

Luz MS, Oliveira PV (2011) Chromium speciation in waters using silica nanoparticles organofunctionalized with APTES and graphite furnace atomic absorption spectrometry. Br J Anal Chem 4:194–200

Mohamed NA, El-Ghany NAA (2017) Pyromellitimide benzoyl thiourea cross linked carboxymethyl chitosan hydrogels as antimicrobial agents. Int J Polym Mater Polym Biomater 66:861–870. https://doi.org/10.1080/00914037.2017.1280794

Nascimento RF, Lima ACA, Vidal CB, Melo DQ, Raulino GSC (2014) Adsorção: Aspectos teóricos e aplicações ambientais. Fortaleza, Brazil

Norouzi S, Heidari M, Alipour V, Rahmanian O, Fazlzadeh M, Mohammadi-moghadam F, Nourmoradi H, Goudarzi B, Dindarloo K (2018) Preparation, characterization and Cr(VI) adsorption evaluation of naOH-activated carbon produced from date press cake; an agro-industrial waste. Bioresour Technol 258:48–56. https://doi.org/10.1016/j.biortech.2018.02.106

Pang L, Hu J, Zhang M, Yang C, Wu G (2018) An efficient and reusable quaternary ammonium fabric adsorbent prepared by radiation grafting for removal of Cr(VI) from wastewater. Environ Sci Pollut Res 25:11045–11053. https://doi.org/10.1007/s11356-018-1355-1

Paulino AT, Belfiore LA, Kubota LT, Muniz EC, Almeida VC, Tambourgi EB (2011a) Effect of magnetite on the adsorption behavior of Pb(II), Cd(II), and Cu(II) in chitosan-based hydrogels. Desalination 275:187–196. https://doi.org/10.1016/j.desal.2011.02.056

Paulino AT, Belfiore LA, Kubota LT, Muniz EC, Tambourgi EB (2011b) Efficiency of hydrogels based on natural polysaccharides in the removal of Cd^{2+} ions from aqueous solutions. Chem Eng J 168: 68–76. https://doi.org/10.1016/j.cej.2010.12.037

Pereira AGB, Martins AF, Paulino AT, Fajardo AR, Gilherme MR, Faria MGI, Linde GA, Rubira AF, Muniz EC (2017) Recent advances in designing hydrogels from chitin and chitin-derivatives and their impact on environmental and agriculture: a review. Rev Virtual Quim 9:370–386

Ravikumar KVG, Kumar D, Rajeshwari A, Madhu GM, Mrudula P, Chandrasekaran N, Mukherjee A (2015) A comparative study with biologically and chemically synthesized nZVI: applications in Cr(VI) removal and ecotoxicity assessment using indigenous microorganisms from chromium-contaminated site. Environ Sci Pollut Res 23:2613–2627. https://doi.org/10.1007/s11356-015-5382-x

Redlich O, Peterson DL (1959) A useful adsorption isotherm. J Phys Chem 63:1024–1026. https://doi.org/10.1021/j150576a611

Sharma A, Bhattacharyya KG (2005) Adsorption of chromium(VI) on Azadirachta Indica (neem) leaf powder. Adsorption 10:327–338. https://doi.org/10.1007/s10450-005-4818-x

Sips R (1948) Combined form of Langmuir and Freundlich equations. J Chem Phys 16:490–495

Tang N, Niu C, Li X, Liang C, Guo H, Lin L, Zheng C, Zeng G (2018) Efficient removal of Cd^{2+} and Pb^{2+} from aqueous solution with amino- and thiol- functionalized activated carbon: isotherm and kinetics modeling. Sci Total Environ 635:1331–1344. https://doi.org/10.1016/j.scitotenv.2018.04.236

USEPA, United States Environmental Protection Agency (2012) Basic information about chromium in drinking water. http://water.epa.gov/drink/contaminants/basicinformation/chromium.cfm (Acessed 24 May 2018)

Varnier K, Vieira T, Wolf M, Belfiore LA, Tambourgi EB, Paulino AT (2018) Polysaccharide-based hydrogels for the immobilization and controlled release of bovine serum albumin. Int J Biol Macromol 120:522–528. https://doi.org/10.1016/j.ijbiomac.2018.08.133

Vieira RM, Vilela PB, Becegato VA, Paulino AT (2018) Chitosan-based hydrogel and chitosan/acid-activated montmorillonite composite hydrogel for the adsorption and removal of Pb^{2+} and Ni^{2+} ions accommodated in aqueous solutions. J Environ Chem Eng 6: 2713–2723. https://doi.org/10.1016/j.jece.2018.04.018

Wan Z, Li M, Zhang Q, Fan Z, Verpoort F (2018) Concurrent reduction-adsorption of chromium using m-phenylenediamine-modified magnetic chitosan: kinetics, isotherm, and mechanism. Environ Sci Pollut Res 25:17830–17841. https://doi.org/10.1007/s11356-018-1941-2

Wu Y, Cha L, Fan Y, Fang P, Ming Z, Sha H (2017) Activated biochar prepared by pomelo peel using H3PO4 for the adsorption of hexavalent chromium: performance and mechanism. Water Air soil Pollut. https://doi.org/10.1007/s11270-017-3587-y

Yusuff AS, Gbadamosi AO, Lala MA, Ngochindo JF (2018) Synthesis and characterization of anthill-eggshell composite adsorbent for removal of hexavalent chromium from aqueous solution. Environ Sci Pollut Res. https://doi.org/10.1007/s11356-018-2075-2

Zhu L, Wang L, Xu Y (2017) Chitosan and surfactant co-modified montmorillonite: a multifunctional adsorbent for contaminant removal. Appl Clay Sci 146:35–42. https://doi.org/10.1016/j.clay.2017.05.027